FRAP in pharmaceutical research: practical guidelines and applications in drug delivery

Hendrik Deschout[1,2], Koen Raemdonck[1], Jo Demeester[1], Stefaan C. De Smedt[1,*], Kevin Braeckmans[1,2,*]

[1]Laboratory of General Biochemistry and Physical Pharmacy, Ghent University, Belgium

[2]Center for Nano- and Biophotonics, Ghent University, Belgium

*Corresponding authors: Stefaan.DeSmedt@UGent.be, Kevin.Braeckmans@UGent.be

ABSTRACT

Fluorescence recovery after photobleaching (FRAP) is a fluorescence microscopy technique that has attracted a lot of interest in pharmaceutical research during the last decades. The main purpose of FRAP is to measure diffusion on a micrometer scale in a non-invasive and highly specific way, making it capable of measurements in complicated biomaterials, even *in vivo*. This has proven to be very useful in the investigation of drug diffusion inside different tissues of the body and in materials for controlled drug delivery. FRAP has even found applications for the improvement of several medical therapies and for the field of diagnostics. In this review, an overview is given of the different applications of FRAP in pharmaceutical research, together with essential guidelines on how to perform and analyse FRAP experiments.

1 INTRODUCTION AND HISTORICAL OVERVIEW

Being able to measure the diffusion of molecules and nanoparticles inside biological or artificial materials has always been of great interest in the life sciences and particularly in pharmaceutically oriented research. This for instance applies to the development of drug delivery systems that should release encapsulated drugs at the right time. Characterization of molecular diffusion inside these systems is required for optimization of their structure and composition. After *in vivo* administration, the therapeutic molecules should be able to diffuse inside tissue where the extracellular matrix (ECM) may act as a barrier so that they do not efficiently reach their target site. As such, a good understanding of the diffusion inside the ECM is required to identify ways of achieving optimal mobility. In some cases, the therapeutics should reach the interior of target cells, so that it is of equal interest to measure the diffusion in the intracellular environment.

Fluorescence recovery after photobleaching (FRAP) is an interesting technique for these purposes, as it is fast, non-invasive, highly specific, and relatively easy to perform. FRAP is a fluorescence microscopy method, requiring that the species of interest, which can be molecules or nanoparticles, are labelled with fluorophores. As illustrated in Figure 1, a FRAP experiment starts by applying a high intensity light beam for a short period of time to a microscopic region inside the sample. This destroys the fluorescent property of the fluorophores in that region, a phenomenon called photobleaching. Immediately afterwards, the fluorescence in the photobleached region will start to recover, because diffusion causes some of the photobleached molecules to leave and other fluorescent molecules to enter. This recovery is monitored by means of a fluorescence microscope and afterwards a suitable mathematical model is used for analysis, generally yielding the fraction of molecules that are mobile and their diffusion coefficient.

FRAP was developed in the 1970s, using specialized microscope set-ups featuring a stationary (i.e. non-scanning) focused light beam for bleaching and a photo multiplying tube (PMT) or avalanche photodiode (APD) for the fluorescence recovery detection (1). As illustrated in Figure 2, for bleaching, the full intensity of the light source was used, while for imaging the light intensity was strongly attenuated. The shape of the photobleached region was restricted to a circular spot with a Gaussian- or uniform-like intensity distribution. Due to the stationary light beam, no spatial information was available of the recovery process and only the total fluorescence in the bleached spot was measured as a function of time. The first applications of FRAP were mainly situated in the field of cell biology, in particular for measuring the diffusion of proteins in the cell membrane (2, 3).

A couple of years later, FRAP was also reported to be used for protein diffusion measurements inside the cell (4, 5). At this time, some groups started to replace the PMT or APD by a camera that was able to capture two-dimensional images of the fluorescence recovery. The additional spatial information could be exploited to analyze the recovery in terms of anisotropic diffusion as well, rather than being limited to isotropic diffusion only (6). At the end of the 1980s, it was shown that FRAP could be applied for diffusion measurements *in vivo* (7). The first pharmaceutical applications of FRAP were reported in the early 1990s, when it was applied for measuring the diffusion rate of proteins inside artificial and biological hydrogels, which is of interest for the development of drug delivery systems (8, 9). Some groups were adapting the mathematical FRAP models for measuring binding instead of diffusion in the cell membrane (10), thus allowing to assess the binding affinity of drug delivery systems for target cell receptors on the plasma membrane.

In the 1990s, user-friendly confocal laser scanning microscopes (CLSMs) became more widespread. This type of microscope can be equipped with an acousto optic modulator (AOM) or an acousto optic tunable filter (AOTF), which allows to change the intensity of the scanning laser beam on a pixel by pixel basis in the image. Thus, as illustrated in Figure 2, arbitrary patterns could easily be photobleached using standard CLSM equipment (11, 12). Another instrumental development that had important consequences for FRAP in pharmaceutical research was multi-photon fluorescence microscopy. Combining this technique with FRAP allows for diffusion measurements much deeper in tissue than possible with conventional single-photon FRAP (13, 14). At the same time, it became clear that the use of the fluorescent protein had important advantages for FRAP measurements inside cells. Until then, the fluorescently labelled proteins had to be microinjected into the cells, a cumbersome manipulation that can disturb the cell's normal working mechanism. Letting the cell express fluorescent proteins, it became possible to perform completely non-invasive FRAP measurements inside cells (15-17). The combination of all these developments resulted in a steep increase in the use of FRAP in the life sciences (18, 19). However, despite the CLSM being able to photobleach complex shapes and to record two-dimensional recovery images, the analysis was usually limited to the total fluorescence of a circular bleached spot. It was only in the 1990s, with enough computer memory and processing power becoming available in standard computers, that FRAP models were developed that started to exploit more of the available spatial information (20, 21). This development is ongoing and allows to extract increasingly more information with better accuracy from the observed fluorescence recovery (22-24).

In this review, the most important practical aspects of FRAP experiments and data analysis will be summarized, followed by a discussion of the different applications of FRAP in pharmaceutically oriented research. Not only pharmaceutically relevant applications will be addressed, like the design and optimization of drug delivery systems, also research will be discussed that is situated more on the interface between pharmacy and medicine, such as the improvement of medical therapies and the development of diagnostic tests.

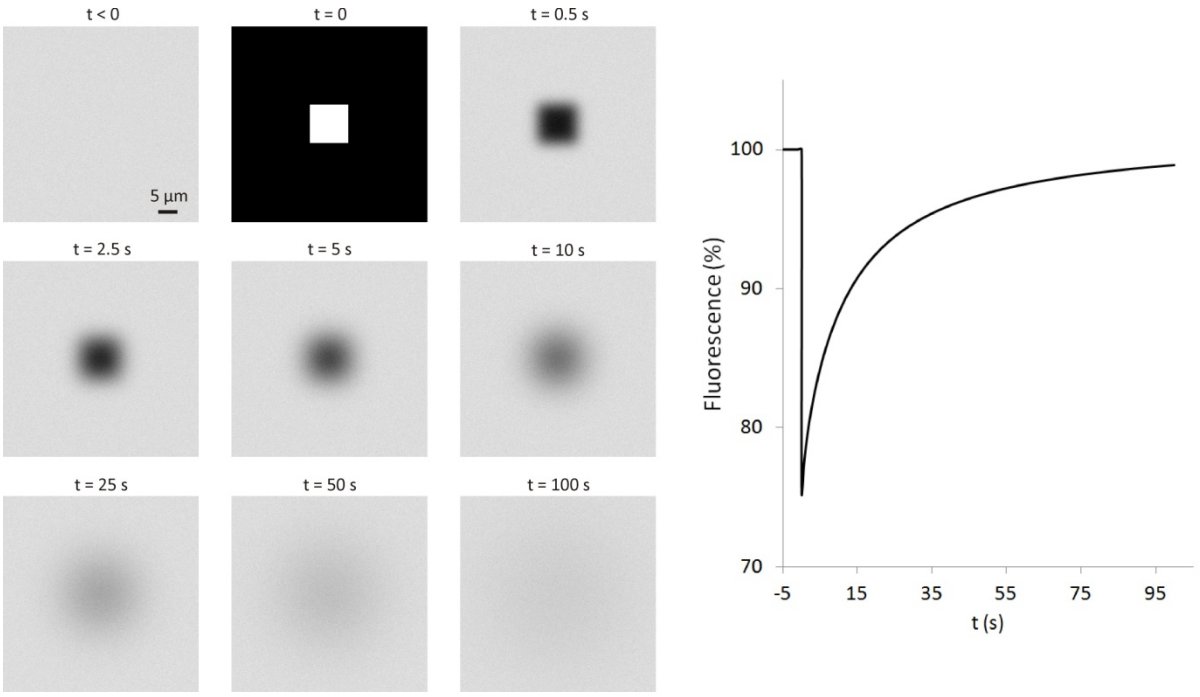

Figure 1: An illustration of a FRAP experiment, showing fluorescence microscopy images at different time points t on the left. At t < 0, before the photobleaching, the initial fluorescence intensity is registered. At t = 0, a square region of 10 µm by 10 µm is photobleached in the center of the image by a high intensity laser beam. In the images at the different time points t > 0 the recovery of the fluorescence inside the photobleached area is visible. On the right, the total fluorescence in the photobleached square normalized to the initial fluorescence is shown in function of time.

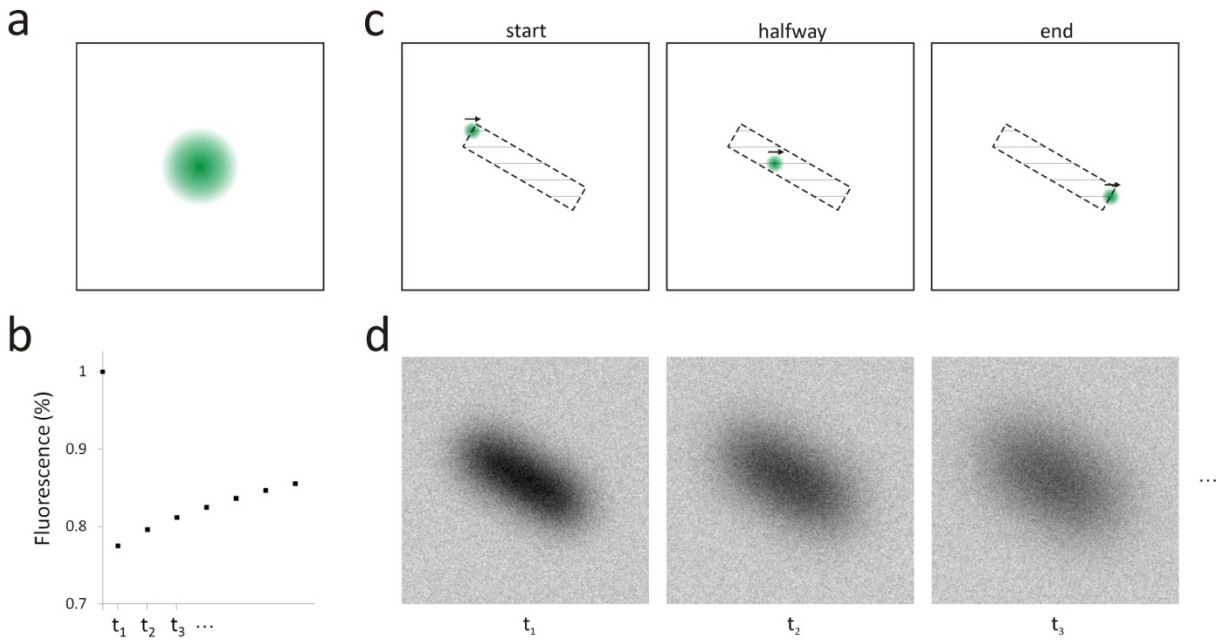

Figure 2: Illustration of a FRAP experiment using a stationary light source and the scanning beam of a CLSM. (a) A stationary light source can only be used to photobleach a circular region. (b) Detection of the fluorescence recovery with a stationary light source is limited to recording the total intensity in the photobleached spot at different time points t_1, t_2, t_3, ... after photobleaching. (c) In case of a CLSM, arbitrary patterns can be photobleached by scanning the laser beam over the image and applying full laser intensity (green spot) inside the pattern and zero intensity outside. (d) Detection of the fluorescence recovery with a CLSM happens by scanning the laser beam with a constant intensity that is attenuated with respect to the photobleaching intensity. This results in 2D images at different time points t_1, t_2, t_3, ... after photobleaching. Thus, not only temporal but also spatial information is obtained.

2 THEORETICAL FRAP MODELS

Although FRAP is a conceptually simple technique, the analysis of the observed fluorescence recovery can be quite involved. Different types of theoretical models have been developed that describe the recovery process in a number of different circumstances. Here, these FRAP models are briefly discussed.

2.1 Diffusion

The original goal of FRAP was to obtain information on the diffusion coefficient of molecules or other nanoparticles, and this is still the most frequent application today. A simple type of analysis is to determine the time it takes until a certain percentage of the fluorescence in the photobleached spot has recovered after photobleaching (25). However, this approach only allows for qualitative comparison of the diffusion coefficient, and requires identical experimental circumstances. A more quantitative type of analysis requires a theoretical model of the recovery process. There are a number of approaches, all starting from the second law of Fick which describes diffusion in the presence of a concentration gradient (26).

2.1.1 *Conventional models*

The first type of FRAP models consisted of a mathematical description of the total fluorescence inside the photobleached spot as a function of the time after photobleaching (see Figure 1). This was an obvious choice, since that was the only signal that could be measured with early instruments where a stationary light beam was used for photobleaching and imaging (1). Fitting the model to the experimental recovery curve yields the diffusion coefficient and the mobile fraction. Nowadays, even with the CLSM as the standard FRAP instrument, this is still common practice. An expression of the total fluorescence recovery inside the photobleached spot can be obtained by solving the second law of Fick with appropriate boundary and initial conditions. For the boundary condition, it is usually assumed that the sample volume is ‘infinitely large’. The initial condition is the concentration profile of the fluorophores immediately after photobleaching, which requires a good description of the photobleaching intensity. Considering a stationary focused laser beam for photobleaching (see Figure 2), the first conventional FRAP models approximated the photobleaching intensity by a circular beam with Gaussian or uniform intensity distribution (1, 27). Similar models have been reported for CLSMs, additionally accounting for the imaging point spread function (PSF) (28). However, the description of the photobleaching intensity is complicated for a CLSM, i.e. the convolution of the scanning motion with the photobleaching PSF (see Figure 2). Models have been developed that describe the total fluorescence recovery inside a photobleached disk, assuming a Gaussian distributed photobleaching PSF that is identical to the imaging PSF (29). This approach has been extended for multi-photon FRAP as well (14).

2.1.2 *Spatially resolved models*

A lot of information is lost by integrating all fluorescence in the photobleached spot, rather than using the full spatial information that is available in the fluorescence recovery images. This limits the analysis in practice to the identification of a diffusion coefficient and a mobile fraction. More complicated situations, like multiple diffusing species, anisotropic diffusion, or flow can be more accurately detected by using the spatial information as well. This can be done by fitting a spatially resolved model to the observed 2D fluorescence recovery. One of the first reports considered the photobleaching of a uniform disk with a CLSM (30). Similar methods were developed for a line and point source (31) or a Gaussian distribution (28) as initial profiles of the fluorophore concentration after photobleaching. A flexible and accurate spatially resolved model was recently developed making use of a photobleached rectangle that can have any size or aspect ratio (22).

2.1.3 *Numerical models*

The analytical models described in Sections 2.1.1 and 2.1.2 are quite convenient, as they only require to perform a best fit of a mathematical formula to the experimental recovery data. In order for these models to be valid, it is important to realize that they are derived for particular conditions to which the experiment should comply. In practice, however, this is sometimes difficult, if not impossible, to achieve. For instance, the sample might not be 'infinitely large' but quite limited, such as when performing FRAP experiments in cells. Problems might also arise when diffusion occurs during the photobleaching phase, which is typically not accounted for in the theoretical models. Also, non-linear effects during the high intensity photobleaching phase, may cause substantial deviation of the photobleached area from the theoretically assumed geometry (32). In these situations that are mathematically complex, only numerical solutions of the second law of Fick might provide a solution, an approach that started to draw attention as soon as standard computers became equipped with sufficient processing power and memory. In a first attempt, the recovery of the average fluorescence of a photobleached line obtained by a CLSM was numerically modelled, incorporating the photobleaching PSF as a Gaussian distribution (33). However, this method still assumes a specific photobleached shape. This limitation was circumvented by using the first image after photobleaching as the initial condition in order to numerically solve the second law of Fick (34). In that way, several diffusion coefficients could be included in the analysis. In similar work, a radially symmetric and non-decreasing initial photobleached profile was assumed, which could be estimated from the first image after photobleaching (23). The drawback of this type of approach is that it requires specific programming expertise that might be too involved for the non-expert user.

2.1.4 *Transform models*

Besides the numerical models (see Section 2.1.3), making use of the Fourier transform of the recovery images is another approach that does not require an analytical description of the initial fluorophore concentration directly after photobleaching (8, 21). This framework has been extended

to incorporate anisotropic diffusion (21). The disadvantage is that a constant fluorophore concentration at the edges of the images is assumed, restricting the size of the photobleached region. In a related effort, the properties of the Hankel transform have been used to distinguish multiple components of diffusion coefficients (24).

2.2 Binding

Besides diffusion (see Section 2.1), also information on the binding kinetics can be derived from the fluorescence recovery in FRAP experiments. Usually, a reversible first order reaction is assumed, described by two partial differential equations, one for the concentration of the diffusing fluorophores and one for the concentration of the bound fluorophores (10, 35). Just like the conventional FRAP models for diffusion (see section 2.1.1), these equations are solved for the total fluorescence recovery over the photobleached spot, considering initial and boundary conditions. Besides the concentration of the diffusing fluorophores directly after photobleaching as initial condition, it is also assumed that the system is in equilibrium before photobleaching. Three different regimes can be distinguished from each other (35). If free diffusion is dominant, the binding can be ignored and the problem reduces to the case of diffusion. When the binding events happen much faster than the diffusion, the recovery can still be described by free diffusion, but with a lower effective diffusion coefficient. A third regime can be considered if the diffusion is very fast compared to the binding reaction and to the timescale of the FRAP measurement. In this case, diffusion is not detected, and the fluorescence recovery is completely determined by the values of the binding rate. The reader is referred elsewhere for more information on this topic (35, 36).

3 GUIDELINES FOR FRAP EXPERIMENTS

Most FRAP models are specific solutions of the second law of Fick (see Section 2). The way a FRAP experiment is performed thus has important consequences for the validity of the chosen model. Here, some general guidelines for FRAP experiments are given.

3.1 Fluorescent labelling

Since FRAP is a fluorescence microscopy technique, the molecules or nanoparticles of interest should be labelled with fluorophores. It is important that the type of fluorophore is small enough, so that it does not significantly influence the diffusion of the labelled molecule or nanoparticle. Additionally, the dye has to have the property that it photobleaches relatively easily. One of the most commonly used dyes for FRAP is fluorescein or its derivative fluorescein isothiocyanate (FITC). In the case that protein mobility inside a living cell is investigated, the use of the green fluorescent protein (GFP) or a variant is mostly used nowadays. Fluorophores that do not photobleach, but instead switch from a dark state to a bright one (photoactivation) or convert from emission in one spectral band to a different one (photoconversion) can also be used for FRAP (37).

One of the basic assumptions in most FRAP models concerning the fluorescent labelling is that the observed fluorescence scales linearly with the concentration of fluorophores. In a FRAP experiment, this generally means that the fluorophore concentration should be low enough, so that fluorescent light emitted by one fluorophore is not likely to be absorbed by neighbouring fluorophores (38). If at all possible it is strongly advised to check linearity of the fluorescence signal by making an appropriate dilution series of the fluorescent probe and determine the maximum concentration that is allowed to be used.

3.2 Photobleaching

The essential part of a FRAP experiment is the photobleaching of a region in the fluorescent sample. The validity of conventional and spatially resolved FRAP models (see Section 2.1.1 and 2.1.2) is crucially dependent on the way this is done, since the photobleached spot determines the initial condition for solving the second law of Fick.

3.2.1 *Light source*

A high intensity light source with a wavelength suitable for absorption by the fluorophores is required for photobleaching. Although originally the focused light from a xenon or mercury light bulb was used, nowadays preference is given to lasers which offer a high intensity collimated beam at a specific wavelength. The argon ion gas laser is popular, because it exhibits high intensity laser lines around 488 nm and 514 nm. However, these lasers are being replaced by smaller and more

convenient solid state alternatives that are becoming available with increasing power. High intensity pico- or femtosecond pulsed laser sources are capable of two-photon photobleaching, in which case the wavelength should be twice the fluorophore absorption wavelength (39). The titanium-sapphire laser that has a tunable wavelength in the range of 700 - 1000 nm is often used in combination with green fluorescent dyes. Although the light source should be intense enough to induce photobleaching, care should be taken to avoid non-linear effects that are not considered by most FRAP models (32).

3.2.2 *Spot shape and size*

Most conventional and spatially resolved FRAP models require a specific shape of the photobleached spot. When a stationary focused light source is used, the models that assume a Gaussian shape can be used, although in practice it is often very difficult to determine the exact width of the spot as it depends on many variables, including the laser intensity, type of fluorophore and the chemical nature of the sample (32). Yet, accurate knowledge of the spot size is of crucial importance as the calculated diffusion coefficient depends on the square of the spot size. Also, care should be taken when the photobleaching is done by a CLSM. The initial condition is then described by the convolution of the photobleaching PSF with the pattern that is scanned by the CLSM. Many FRAP models ignore the influence of the photobleaching PSF, but this is only permissible if the photobleached spot is sufficiently large (i.e. five times larger than the standard deviation of the photobleaching PSF) (29).

The actual shape of the photobleached spot can deviate from the intended shape because of a significant amount of recovery already taking place during photobleaching, which is not accounted for by most conventional FRAP models (40). When the model does not correct for this effect, the time it takes for photobleaching should be minimized as much as possible. Photobleaching by long exposure or by repeating the photobleaching step several times should thus be avoided. As a rule of thumb, the photobleaching time is usually taken to be at least 15 times smaller than the characteristic recovery time, that is defined as the average time it takes for a molecule or nanoparticle to diffuse from the center to the edge of the spot (18). The effect of recovery during photobleaching can thus also be limited by increasing the size of the photobleached spot.

3.2.3 *Objective lens*

In case of a high numerical aperture (NA) objective lens (e.g. NA = 1.2), the photobleached volume in the direction of the optical axis is not uniform, but has a distinct conical shape and concentration gradient, meaning that recovery along this direction cannot be ignored, see Figure 3. The only exception is the specific case of molecules or nanoparticles that diffuse in a 2D plane (e.g. in the cell membrane). That is the reason why low NA objective lenses (e.g. NA = 0.2) are often used in FRAP, since these have a low axial resolution that distributes the photobleaching light intensity over an extended cylindrical profile along the optical axis (see Figure 3). The drawback of low NA objective lenses for photobleaching is of course the low resolution, which results in less detailed recovery

images. A more cylindrical profile can also be obtained with a high NA objective lens in case there is an adjustable beam expander in the excitation beam path of the microscope. This allows underfilling of the back aperture of the objective lens so as to obtain a lower effective NA for illumination.

Regardless of the objective lens NA, the effect of recovery in the direction of the optical axis is even stronger in multi-photon than in single-photon FRAP, requiring specialized models (14). However, the obvious advantage of multi-photon compared to single-photon FRAP is that photobleaching can be achieved much deeper in the sample, as the wavelength of the excitation light is situated in the infrared range. An alternative approach to perform FRAP experiments deep in tissues is the microfiberoptic epifluorescence photobleaching (MFEP) method (41). In MFEP, photobleaching happens by a multimodal optical fiber with a micron sized tip that is introduced deep inside the sample.

3.3 Fluorescence recovery

After photobleaching, the fluorescence recovery is monitored in a FRAP experiment. The way this is done and the nature of the recovery both affect the validity of the selected FRAP model.

3.3.1 *Detection of the recovery*

The recovery of the fluorescence is usually monitored at several time points fast enough after photobleaching so that the beginning of the recovery is captured in detail. As a rule of thumb, the time interval between these different time points is taken to be three times smaller than the characteristic recovery time (see Section 3.2.2). If there is an immobile fraction present, enough time points should be included so that recovery in a later stage is also monitored.

However, photobleaching during detection of the fluorescence recovery can alter the apparent recovery kinetics, as illustrated in Figure 4. A balance is, therefore, needed between the number of time points (i.e. the amount of recorded images) and the photobleaching during imaging. This effect can be corrected for, either by including it explicitly in the FRAP model (42), or by monitoring the fluorescence of a suitable background region in the recovery images. The second option is of course only possible with instruments such as a CLSM that acquire images that cover a significantly larger field of view than the photobleached spot. This solution has the advantage that it also corrects for possible intensity fluctuations during imaging.

3.3.2 *Deviations from ideal recovery*

Many FRAP models consider only one diffusing species, sometimes in combination with an immobile fraction. If flow is present, the recovery will occur faster than would be expected based on diffusion alone, leading to an overestimation of the real diffusion rate. Care should therefore be taken to avoid flow in the sample, although theoretically it can be taken into account (1). The latter option is generally not preferred when only the measurement of diffusion is of interest, as it increases the

number of parameters that need to be fitted and thus decreases the precision with which they can be calculated. Related to this, the sample should be in thermodynamic equilibrium so that no net mass transport is occurring that would distort the FRAP measurement. In case of deviations from simple one-component diffusion, e.g. anomalous diffusion or multiple diffusing species, a specialized FRAP model should be applied.

Almost all FRAP models assume that the sample has an infinite volume as boundary condition. In practice, this means that the diffusing molecules or nanoparticles should not be hindered during the monitoring of the fluorescence recovery. Deviations from this boundary condition should be avoided as much as possible, which is especially a concern inside cells.

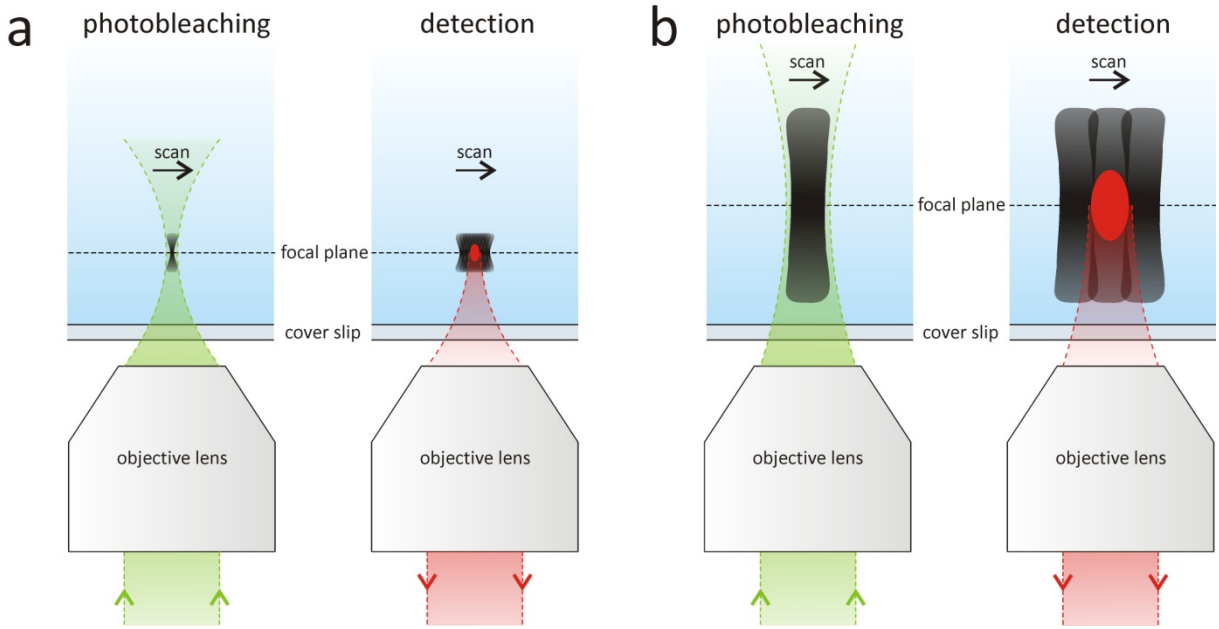

Figure 3: An illustration of the effect of the numerical aperture of the objective lens on the shape of the photobleached volume when using a CLSM. (a) For high numerical apertures, the extension of the photobleached volume in the direction of the optical axis is limited, meaning that fluorescence recovery in that direction cannot be ignored. (b) In case of a low numerical aperture, the photobleached volume is much more extended in the direction of the optical axis, which allows to ignore the fluorescence recovery in that direction.

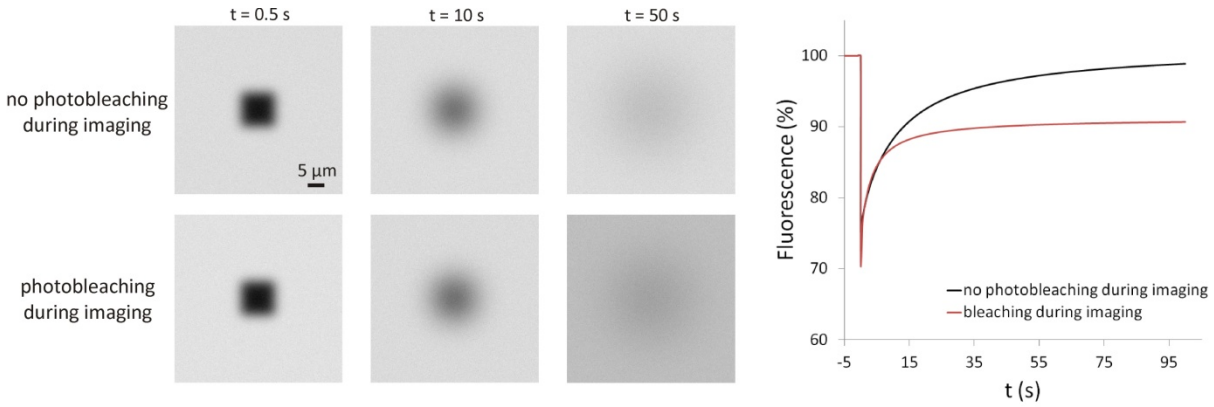

Figure 4: An illustration of the effect on photobleaching during imaging on a FRAP experiment. On the left, fluorescence microscopy images at three different time points t after photobleaching are shown, for both the situation of photobleaching and no photobleaching during imaging. At t = 0, a square region of 10 µm by 10 µm is photobleached in the center of the image. On the right, the total fluorescence in the photobleached square as normalized to the fluorescence before photobleaching is shown for both situations in function of time. When the photobleaching during imaging is not corrected for, the observed fluorescence recovery is distorted.

4 APPLICATIONS OF FRAP IN PHARMACEUTICAL RESEARCH

4.1 Designing drug delivery systems

Drug delivery systems are being developed to achieve time-controlled delivery of encapsulated drugs. Apart from drug solubility, diffusion in these systems is an important factor that contributes to the effective drug release rate. FRAP allows to measure diffusion within drug delivery systems, thus providing important information for optimization of their structure and composition.

4.1.1 *Diffusion inside hydrogels*

Hydrogels comprise an important class of matrix materials for time-controlled drug delivery. A hydrogel consists of a physically or chemically cross-linked 3D network of hydrophilic polymers that has absorbed a large amount of water (43). Drug molecules can be trapped in the hydrogel by chemical bonds and hydrophobic or electrostatic interactions. Dependent on the mesh size of the polymeric network, some therapeutic molecules (e.g. pharmaceutical proteins) can be physically trapped in the hydrogel pores. This not only shields the molecules from the environment, but also allows to tailor drug release from the hydrogel matrix The drug release is often mediated by a gradual degradation and/or swelling of the hydrogel network (44). FRAP has proven to be a valuable technique for characterization of the diffusion process underlying the overall release profile. In this type of studies, often fluorescently labelled dextrans (e.g. FITC-dextrans) are used as a model for drug molecules like peptides and proteins, as they are available in a large range of molecular weights with a variety of fluorescent labels.

Various techniques and polymers have been used to fabricate hydrogels for drug delivery. One example is the use of peptide sequences that fold and self-assemble into hydrogels (45). FRAP measurements showed that the mobility and release of dextrans could be modulated by varying the mesh size. Another self-assembling hydrogel was based on biodegradable dextran microspheres (46). The hydrogel was obtained by hydration of mixtures of oppositely charged dextran microspheres with a protein solution. FRAP was used to study the mobility of proteins in these gels, showing a continuous release of entrapped proteins with preservation of their activity.

Other preparation methods exist besides self-assembly, such as step-growth polymerization of poly(ethylene glycol) (PEG) (47). FRAP measurements of dextrans inside these gels corresponded well with results from NMR spectroscopy and release experiments. Another PEG-based hydrogel was formed by the radically cross-linkable oligo(poly(ethylene glycol)fumarate) together with two cross-linking agents (48). FRAP experiments were performed to measure the diffusion coefficient of dextrans inside this hydrogel. Hydrogels have also been fabricated by chemically cross-linking 1.5 wt % chitosan with dialdehydes (49). FRAP was used to measure the diffusion of dextrans with different molecular weight in these hydrogels and in aqueous solution. Above a molecular weight of 100 kDa, the relative diffusion of dextrans in the gel versus water was found to decrease, suggesting the onset of hindered diffusion because of the cross-linked polymer mesh of the gel.

Composite hydrogel systems have also been of interest, such as agarose-dextran composite gels (50). FRAP was used to measure diffusion of proteins and polysaccharides in these hydrogels and in aqueous solution, indicating an increase in hindered diffusion with hydrodynamic diameter. Additionally, the diffusion was more hindered in hydrogels with higher dextran concentrations. Another example are gelatin hydrogels in which chondroitin sulfate (ChS) was incorporated to retard the release of cationic proteins because of electrostatic interactions (51). FRAP showed that diffusion of lysozymes inside the hydrogel increases with increasing ChS content.

More complicated fabrication processes allow for greater flexibility in hydrogel properties. Hydrogels consisting out of ABA triblock copolymers were fabricated, in which the A-block is a thermosensitive polymer and the B-block is a PEG (52). The gels were prepared by thermogelling combined with photopolymerization, which is a fast and simple cross-linking method that improves stability and mechanical properties. FRAP showed that the release rate of bovine serum albumin (BSA) depended on the protein size and the hydrogel molecular weight between the cross-links. In related work, FRAP was used to measure the diffusion of dextrans in the same type of hydrogel for different temperatures used during thermogelling (53). The diffusion and mobile fractions were found to decrease upon elevating the temperature above 25° C, and the mobility could be adjusted by changing the PEG block length.

Complicated hydrogel fabrication can lead to interesting hydrogel structures. For instance, hydrogels with nanostructured porosity were produced by synthesizing and cross-linking ABA triblock copolymers, with ε-caprolactone (PCL) A-blocks and a poly(ethylene oxide) (PEO) B-block (54). By subsequently degrading the gels by hydrolysis to remove the PCL domains, pores are formed which allow fast transport of molecules through the hydrogel. By using FRAP, it was shown that diffusion of proteins and polystyrene beads inside the hydrogel is higher than in comparable homogeneous hydrogels.

Intelligent stimuli-sensitive hydrogels that change behaviour in response to varying environmental conditions have also been developed. A hydrogel for colon drug delivery was fabricated, using an enzymatic procedure to modify a galactomannan hydrogel and guar oligomer in order to entrap the guar oligomer (55). The hydrogel retains the guar oligomer until it reaches the colonic environment where bacteria-secreted enzymes degrade the hydrogel. FRAP was used to quantify the diffusion of guar oligomer inside the hydrogel, showing that diffusion was decreased significantly compared to non-interacting probes and remained constant over a couple of hours, resulting in a gradual release. Another system intended for colonic drug delivery is a hydrogel based on konjac glucomannan, which is a polysaccharide that is not degradable in the small intestine but is degradable by anaerobic human intestinal bacteria (56). FRAP was performed to measure the diffusion and mobile fraction of dextrans in the system and it was found that the diffusion behaviour cannot only be explained by macroscopic properties of the medium. Also the molecular size and a sieving mechanism have to be taken into account.

4.1.2 *Permeability of polyelectrolyte capsules*

Layer-by-Layer (LbL) polyelectrolyte capsules are microparticles that are being evaluated for controlled drug delivery (57). The polyelectrolyte shells of the capsules are semi-permeable, so that

large molecules cannot diffuse through the polymer wall, resulting in their protection from environmental degradation. In this context, FRAP has been used assess the permeability of the capsule walls by monitoring the fluorescence recovery after completely photobleaching the fluorescence inside the capsule.

Different methods have been investigated to load molecules inside LbL polyelectrolyte capsules. For instance, in the case of capsules that consist of eight layers of poly(diallyldimethylammonium chloride) and poly(styrene sulfonate), this could be done by temperature induced rearrangements within the shells (58). FRAP was used to demonstrate that the permeability for dextrans decreases after heat incubation. Another example are composite systems composed of poly-L-lysine and trisodium citrate LbL polyelectrolyte capsules that contain magnetic particles (59). Using FRAP, it was found that the permeability for dextrans could be controlled by altering the extent of glutaraldehyde cross-linking. It has been argued that polysaccharides offer an attractive biocompatible alternative over synthetic polyelectrolytes. For instance, the anionic alginate sodium and cationic chitosan were used as wall components for multilayer LbL capsules (60). The shells displayed high stability in poly(styrenesulfonate sodium) and FRAP was used to study the permeability of the shells.

4.2 Overcoming drug delivery barriers

When soluble drugs or drug-loaded nanoparticles (i.e. nanomedicines) are administered to the human body, they need to manoeuvre inside ECMs before they reach their target cells. A variety of ECMs exist, which have in common that they are rather complex materials that consist of networks of biomacromolecules that can hinder the transport of drugs, and thus act as a barrier for drug delivery. As illustrated in Figure 5, FRAP has been used to measure the mobility in these ECMs, information that is useful in the design of carriers for drugs that could assist them to reach their destination.

4.2.1 *Solutions and gels as model ECM*

Different types of gels and solutions have been used as a model to study mobility in ECMs. One example is agarose gel and simulated tissue consisting of cells embedded in agarose gel (8). FRAP was used to study the diffusion of dextrans and proteins in these gels. In another study, the diffusion of proteins, polystyrene microspheres, dextrans, and dendrimers in PEO and guar galactomannan solutions was measured with FRAP (61). The purpose was to investigate the effect on diffusion of different probe sizes and shapes relative to the PEO and guar galactomannan mesh. It was found that diffusion of nanospheres was more hindered than dextrans with the same hydrodynamic diameter. At equal mesh size, the diffusion through the more rigid guar galactomannan solution was hindered compared to the more flexible PEO solution. Mobility in ECMs was also modelled with cross-linked matrices consisting of the proteins fibrinogen, fibronectin, and concanavalin A (62). The mobility of Texas red and dextrans inside these matrices and in solution was measured with FRAP. Diffusion was found to be 3 to 4 orders of magnitude slower than in solution, and hindered diffusion was observed as well, caused by specific molecular interactions of the probes with the matrix proteins.

4.2.2 *Tumour interstitium*

The tumour interstitium is an important barrier for drug delivery in cancer therapy (63). This ECM consists of a collagen network embedded in a gel of the proteins glycosaminoglycan and proteoglycan. FRAP is a particularly interesting technique in this context, because diffusion is the most important transport mechanism for nanomedicines inside tumours (64).

To investigate the effect of collagen in the tumour interstitium, FRAP was used to measure the diffusion of immunoglobulin (IgG) in different human tumour xenografts in mice (65). The diffusion of IgG was found to decrease with the amount of collagen in the tumour, while collagenase treatment significantly increased diffusion, identifying collagen as an important diffusion barrier for tumour interstitium penetration. A similar investigation was carried out on the effect of different tumour types and anatomical locations on the diffusion rate (64). The diffusion of proteins, dextrans, and liposomes inside two different human tumour xenografts grown in cranial windows and dorsal chambers in mice was investigated with FRAP. Diffusion was faster in the cranial window than in the dorsal chamber tumours, which correlates with a lower density of host stromal cells that synthesize collagen in the cranial window tumours, confirming that collagen plays an important role in diffusion hindrance in the tumour interstitial fluid. To investigate the effect of collagen in more detail, FRAP measurements were carried out on diffusing proteins and dextrans inside collagen gels (66). Good agreement was found with *in vivo* measurements in tumours with a comparable collagen concentration.

More recently, investigations have been undertaken to identify the role of other tumour interstitium properties on the mobility besides collagen content. For instance, the spatial orientation of the collagen network was studied by measuring the diffusion of dextrans inside collagen gels and human tumour xenografts using multi-photon FRAP (67). It was shown that the network orientation leads to diffusion anisotropy, although it does not affect overall diffusion. This was confirmed in another investigation, where two-photon FRAP was used to measure the diffusion of dextrans in collagen gels that were aligned in a magnetic field (68). In the same study, the effect of glycosaminoglycans (e.g. hyaluronan) and proteoglycans (e.g. decorin) was also investigated by adding decorin and hyaluronan to the collagen gels. The presence of decorin had no effect on the diffusion, while high concentrations of hyaluronan increased diffusion. In relation to these findings, the effect of collagen and hyaluronan degrading enzymes on the diffusion of dextrans in human tumor xenografts was investigated (69). FRAP showed that the diffusion increased largely due to the collagen degrading enzymes. Investigation of the difference in diffusion hindrance caused by interstitial versus cellular constituent was also carried out (70). Multi-photon FRAP measurements of the diffusion of IgG in tumours and gels consisting out of collagen and hyaluronan showed that decreasing the cell density increases diffusion.

Although it is possible to perform FRAP in human tumours *in vivo*, it is more convenient to conduct such experiments *ex vivo* on biopsies. To quantify the effect of excision and cooling, FRAP was used to measure the diffusion of BSA and IgM in human tumour xenografts in mice both *in vivo* and *ex vivo* (13). The correction determined from these measurements was applied to calculate the diffusion of BSA and IgM in human tumours *in vivo* from the values obtained in biopsies. A higher diffusion was found in human tumour xenografts *in vivo*, probably because of a lower concentration of collagen in

the accessible regions of human tumours. A solution to this problem is given by the MFEP method (see Section 3.2.3), where a fiber with a micron sized tip is introduced deep inside tissue *in vivo* (71). Inside subcutaneous tumours in mice, the diffusion of dextrans was indeed found to be slower deeper inside the tumour tissue. Other experimental complications such as the effect of flow in tumours have been investigated as well. A method based on multi-photon FRAP has been developed to account for such flow (72). Both diffusion and flow of dextrans were measured in murine tumours implanted in dorsal chambers in mice *in vivo*.

4.2.3 *Brain extracellular matrix*

The brain ECM in which neurons, glial cells, and blood vessels are embedded, consists of ions, neurotransmitters, metabolites, peptides, and other molecules (73). This ECM is an important barrier for drugs that treat diseases and disorders related to the brain function. To enable successful drug delivery to the brain, it is thus important to understand transport inside the brain ECM, for which FRAP can again be useful (74).

For instance, FRAP was applied to measure the diffusion of dextrans in mouse brain *in vivo*, showing that it is threefold slower than in solution (73). In case of seizure activity or cytotoxic brain edema associated with head injury, the diffusion was found to decrease by more than a factor of 10. In a similar study, a drop in diffusion was also found in the presence of cytotoxic brain edema, while a slight increase in diffusion was measured in case of vasogenic brain edema associated with brain tumour (75). However, a fourfold decrease in diffusion was found inside the brain tumour itself. The extent of diffusion hindrance in the brain ECM was investigated in detail by performing FRAP on dextran inside mouse brain ECM and inside solution (76).

To measure diffusion in the ECM in parts of the brain that are not accessible by light microscopes, the MFEP method (see Section 3.2.3) was applied (77). Dextrans were found to diffuse more than 4 times slower in the cerebral cortex ECM compared in solution, independent of the depth inside the cerebral cortex. It was also shown that diffusion varied strongly in different parts of the brain, with faster diffusion in the thalamus and slower in the hippocampus compared to the cerebral cortex. Deep inside the brain, the diffusion compared to free solution was strongly dependent on the dextran size, indicating hindered diffusion, while this was not the case in the cerebral cortex.

4.2.4 *Mucus*

Several epithelial surfaces in mammalian organs in the respiratory, gastrointensital, and reproductive tract are covered with a mucus layer. This layer limits the exposure of human tissues to external pathogens and as such also represents a significant barrier for drugs that have to reach or get across these epithelial linings (78). Mucus is a viscoelastic gel with as main components water, mucin, inorganic salts, carbohydrates, and lipids. The thickness of the mucus layer ranges from a few micron to several hundred microns, depending on the organ. FRAP can be used to study the ability of drugs to diffuse within the mucosal network (79).

FRAP was used to measure the diffusion of immunoglobulin (IgA, IgG, and IgM) inside human cervical mucus (9). It was found that immunoglobulin diffusion was relatively unhindered, suggesting pore sizes in the mucus of around 100 nm. In a similar investigation, FRAP was used to determine the diffusion of proteins, viruses, and polystyrene microspheres in human cervical mucus (80). Most proteins and even the smaller viruses could diffuse as rapidly in mucus as in water. The larger microspheres and viruses did not diffuse, probably because of sticking to mucin strands. In line with these results, a FRAP study in expectorated cystic fibrosis lung sputum (see Figure 5) revealed that the mucus network did not hinder diffusion of dextrans with different molecular weights up to 2000 kDa (corresponding to a hydrodynamic diameter of approx. 65 nm) (29). Taken together, these investigations suggest that mucus does not pose a sterical barrier to molecules or small nanoparticles, although adhesion to the biopolymers might be an issue.

In the context of gene therapy, FRAP was employed to measure diffusion of plasmid DNA in bovine cervical mucus (81). Supercoiled DNA was found to diffuse faster than linear DNA, and complexation of the DNA with liposomes increased the diffusion two-fold.

4.2.5 *Other drug delivery barriers*

For the treatment of bone diseases such as osteoporosis or osteonecrosis, it is essential that drugs are able to traverse the bone tissue. Bone mainly consists out of osteocytes that form a cellular network embedded within a mineralized matrix that is largely impermeable. Instead of diffusion, it is hypothesized that load-induced flow within the bone lacunar-canaliculi system serves as the main transport mechanism in bone (82). FRAP is an interesting technique to gain better understanding of this flow, as it complements the classic perfusion measurements that lack temporal dynamics and that are prone to histologic artefacts (83). The technique was applied to measure the diffusion and flow of sodium fluorescein in the lacunar-canaliculi system of mouse bone, confirming the hypothesis of a load-induced flow (84).

In the treatment of retinal diseases, intravitreal injection is an attractive administration route for drugs, since systemic delivery is impeded by the blood-retina barrier. The vitreous humour is a hydrogel formed by a network of collagen fibrils that are cross-linked by proteoglycan filaments. Besides collagen and proteoglycan, the vitreous also contains other proteins such as hyaluronan. Contrary to the case of cystic fibrosis sputum (see Section 4.2.4), FRAP measurements showed that dextrans in the vitreous experience a sterical hindrance that is proportional to their molecular weight, likely due to the dense network of hyaluronic acid polymers (29). In the context of gene therapy, FRAP has been used to measure the diffusion of polystyrene nanospheres and complexes of plasmid DNA and liposomes in the vitreous of bovine eyes (85). While nanospheres functionalized with PEG were found to be mobile, the DNA complexes were immobilized because of aggregation and binding to fibrillar structures in the vitreous. By adding a PEG coating to the DNA complexes, aggregation and binding could be prevented.

The stratum corneum is the top layer of the skin and consists of several layers of corneocytes. Since its purpose is to protect the underlying tissue, it constitutes the primary barrier for transdermal drug delivery. Mobility measurements inside the stratum corneum are, therefore, of interest in the development of drug formulations intended for topical administration. In this context, FRAP was

used to measure the diffusion of several lipophilic probes of different molecular weight, such as DACM or BOD, in model lipid bilayers and in a lipid bilayer consisting of human stratum corneum extracted lipids (86).

4.3 Drug delivery inside cells

An increasing number of nanomedicines are developed for drug delivery in the intracellular space of target cells, which means they need to find their way inside the cytoplasm, and sometimes even to the cell nucleus. A better understanding of mobility inside the cell is thus of great importance in this effort (19).

FRAP has been used to investigate the diffusion of a variety of macromolecules inside living cells, as illustrated in Figure 6. For instance, the technique was used to measure the diffusion of microinjected dextrans with different molecular weights inside the cytoplasm and nucleus of epithelial cells and fibroblasts (87). The diffusion in both cytoplasm and nucleus was found to be approximately 4 times slower than in water. This factor was independent of the molecular weight up to 500 kDa, indicating that the diffusion is unhindered in this molecular weight range. This result was contradicted by other studies, where FRAP was used to measure the diffusion of dextrans (88) and proteins (89) with different molecular weights in the cytoplasm of muscle cells. The diffusion of the dextrans and especially the proteins was found to be hindered with increasing molecular weight, likely because of different compounds of the cytoskeleton. Recently, FRAP was used to show that the cytoplasm of cells behaves like a poroelastic material (90).

Besides these general investigations, FRAP has also been applied to measure the intracellular diffusion of nucleic acids, which is of relevance to gene therapy. The diffusion of double stranded DNA fragments with different numbers of base pairs was measured after microinjection into the cytoplasm and nucleus of HeLa cells (see Figure 6) (91). In the cytoplasm, diffusion was found to be significantly lower than in water, and the diffusion was found to be increasingly hindered with an increasing number of base pairs. In the nucleus, the DNA fragments were immobile, in contrast to dextrans with similar molecular weight, indicating that DNA immobilization is caused by binding. FRAP was also used to investigate the diffusion of single stranded DNA. For instance, after introduction into the nucleus of rat myoblasts, the diffusion of oligodeoxynucleotides was found to be similar to its diffusion in solution (92).

Potential intracellular drug delivery carriers, such as Tat-derived peptides (93), have also been studied. FRAP was used to investigate the intracellular mobility of Tat-peptides with cargoes of different molecular weights below and above the threshold for diffusion through the nuclear pores (94). This was done by photobleaching the fluorescence inside the nucleus and subsequently monitoring the recovery coming from the cytoplasm, and vice versa. Combined with FRAP diffusion measurements, it was found that the Tat-peptides with cargoes with a molecular weight below the threshold are able to cross the nuclear envelope by diffusion.

4.4 Improving therapy

FRAP can also be of interest for providing information that helps improving medical therapies. FRAP has found a number of different and sometimes surprising applications in this context.

Several neuro-degenerative diseases, such as Parkinson's and Alzheimer's disease, are related to protein or peptide aggregates inside the brain. FRAP has been reported for measuring the diffusion of α-synuclein (95) and amyloid-β (96) aggregates, providing information that is not only useful for a better understanding of the molecular mechanisms that cause these diseases, but also for assessing potential treatments that can reverse this aggregation. Besides these mobility measurements, FRAP has also been employed to assess cell membrane perturbations caused by amyloid-β aggregates (97). This can be done by measuring the membrane fluidity, which basically means verifying whether lipids inside the membrane are undergoing free diffusion or not.

Stem cell therapy is a promising approach for the treatment of a variety of pathologies. In this context, it is important to assess the gap junctional intercellular communication (GJIC), as it is essential for maintaining homeostatic balance and normal differentiation of cells. FRAP was used to measure the presence of GJIC, not by measuring diffusion in the classical sense, but by monitoring the fluorescence recovery rate in one cell due to influx of fluorescence from another cell through the gap junction channels between both cells (98-100).

For cancer therapy, FRAP was used to monitor the change in mobility of tumour associated proteins inside living cells induced by candidate anti-cancer drugs such as dihydroartemisinin (101), apigenin (102), cytosine arabinoside (103), and multimeric RGD-peptides (104). FRAP can also be used to determine binding kinetics, which is useful in the context of cancer therapy in order to assess the binding affinity of antibodies to their tumour-associated antigen (105, 106). FRAP has also been reported to measure the effect of an apoptosis inducing drug on the GJIC (107), and to measure the cell membrane fluidity in the context of electro-chemotherapy (108).

Injury treatment is also of interest in pharmaceutical research and FRAP has found some applications in this context. For instance, the diffusion of dextrans was measured *in vivo* inside blood vessels of injured muscle tissue of mice in order to assess the endothelial barrier function (109). In the context of retinal injuries, the diffusion of dextrans in the retina ECM of mice was measured after damage was induced by elevated intraocular pressure (110). Furthermore, FRAP has been used to study the effect of the antioxidant α-tocopheral on the membrane fluidity after arterial injury (111).

Some specific applications of FRAP have also been reported in the context of a variety of other medical treatments. Pulsed high intensity focused ultrasound is a technique that has potential to treat thrombolysis. FRAP was used to measure the diffusion of dextrans in blood clots after treatment, and it was found that the diffusion coefficient increased significantly (112). In the context of cystic fibrosis, FRAP was used to measure the diffusion of dextrans in the fluid of submucosal glands (113). A decrease in diffusion was found compared to the normal situation, providing evidence for defects in submucosal gland function caused by cystic fibrosis. In research on the human immunodeficiency virus type 1, FRAP was used to determine the effect of sphingomyelinase treatment on the diffusion of several receptor proteins in the cell membrane (114). It was found that the diffusion of the HIV receptor CD4 decreased after treatment. FRAP measurements of diffusion of proteins inside cells were also undertaken in research aimed at improving the treatment of diarrheal diseases (115), neuropsychiatric disorders (116), and obesity (117).

4.5 Diagnostics

A less obvious application of FRAP is situated in the field of diagnostics. Medical conditions are sometimes preceded by a change in the structure of the affected cells or the surrounding ECM. This, in turn, can result in a change of mobility inside these cells or the ECM. In this context, at least one effort has been undertaken to use FRAP as a diagnostic assay by measuring such changes in mobility. The technique was used to measure the diffusion of dextrans dissolved in artificial cerebrospinal fluid that was administered in the ECM of mouse brain *in vivo* after craniectomy. This is of interest since diffusion inside the brain ECM is related to neural activity (73). It was found that slowed diffusion preceded seizure activity, indicating that FRAP measurements can be used as a predictor of impeding brain seizure. However, considering the highly invasive nature of this procedure, the application of FRAP as a diagnostic assay might be limited. A technique like the MFEP method (see Section 3.2.3) might possibly solve this issue in certain situations. In another study, FRAP was used to investigate the diffusion of dextrans inside a tissue-engineered skeletal muscle model in compressed and uncompressed state (118). A significantly reduced diffusion coefficient was found in the compressed state, information that could be helpful in the development of a screening method for early detection of pressure-related deep tissue injuries.

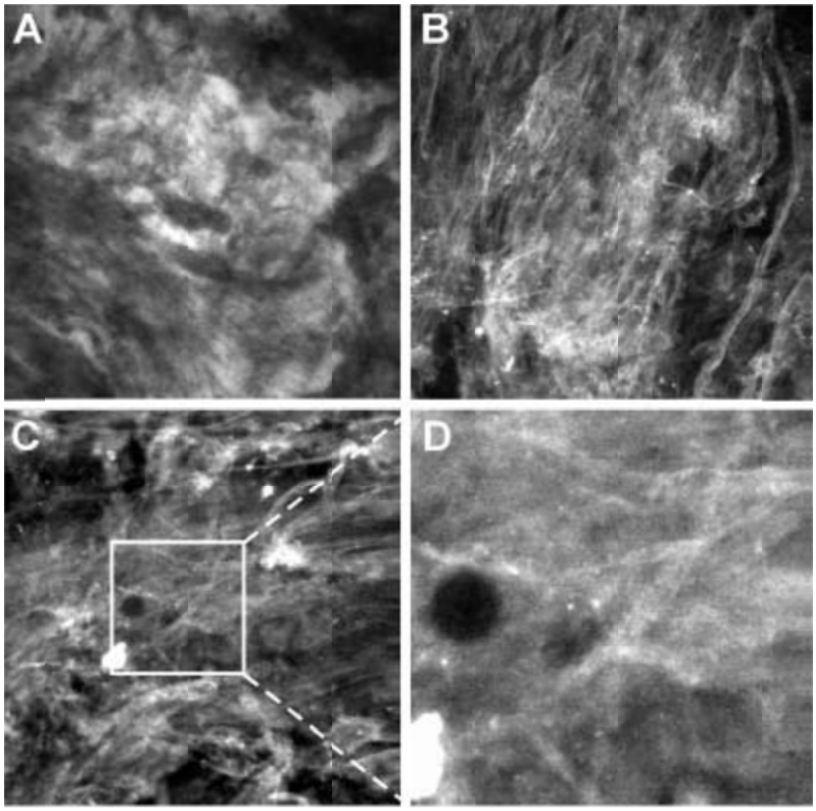

Figure 5: An illustration of the use of FRAP to measure the mobility inside an ECM. (a) Fluorescence microscopy image (1047 μm by 1047 μm) of cystic fibrosis sputum mixed with fluorescently labeled dextrans. (b) Fluorescence microscopy image (1047 μm by 1047 μm) of cystic fibrosis sputum mixed with fluorescently labeled polystyrene nanospheres. (c) Fluorescence microscopy image (524 μm by 524 μm) of cystic fibrosis sputum mixed with fluorescently labeled polystyrene nanospheres after performing a FRAP experiment that involved photobleaching of a disk with a radius of 15 μm. (d) Enlarged part (175 μm by 175 μm) of image (c). The figure is reproduced from reference (29).

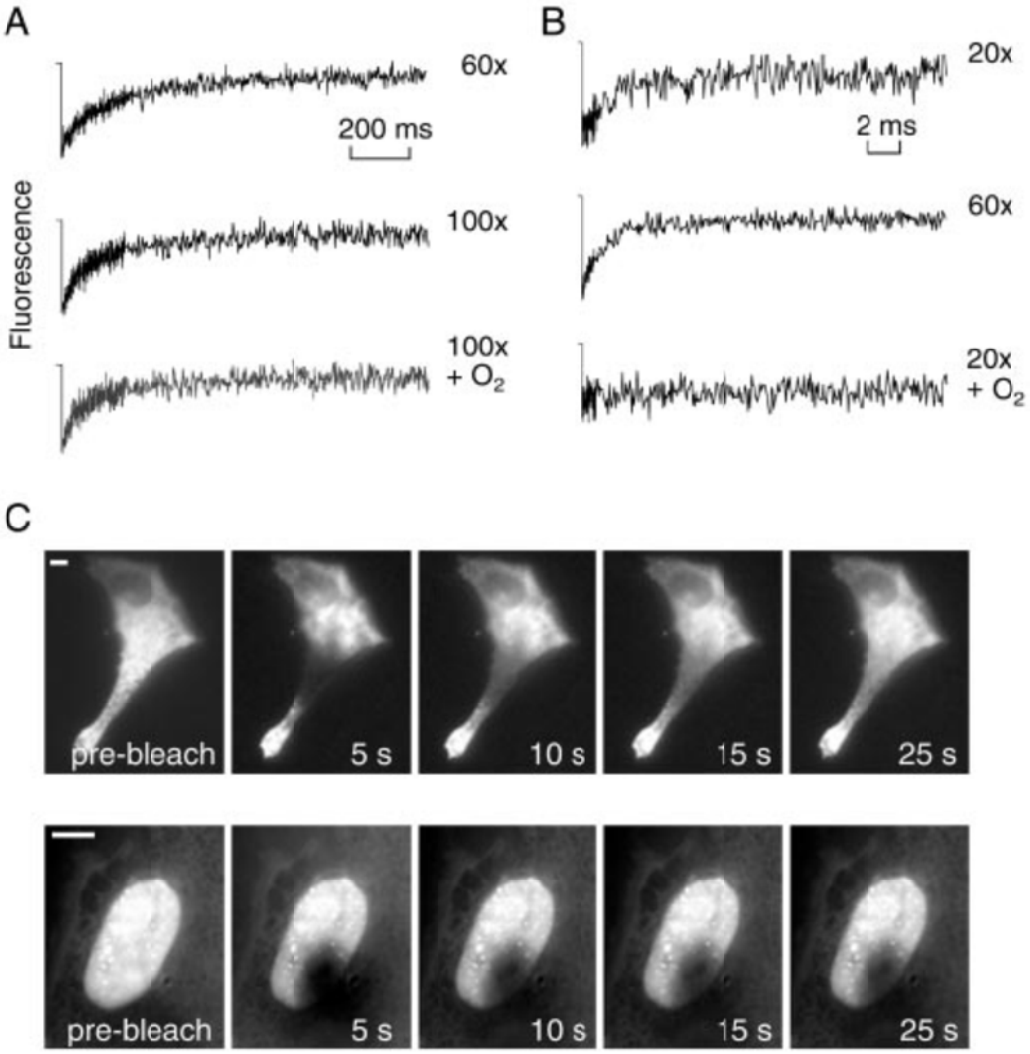

Figure 6: An illustration of the use of FRAP to measure the mobility inside cells. (a) FRAP recovery profiles of labelled DNA in the cytoplasm of cells using a 60× or 100× objective lens (in air or in O_2-saturated solution). (b) FRAP recovery profiles of fluorescently labelled oligonucleotides in the nucleus of cells using a 20× or 60× objective lens (in air or in O_2-saturated solution). (c) Fluorescence microscopy images recorded at different time points showing the recovery of the fluorescence after photobleaching fluorescently labeled DNA in the cytoplasm (top) or nucleus (bottom) of cells. The scale bar is 5 µm. The figure is reproduced from reference (91).

5 CONCLUSION AND FUTURE OUTLOOK

Almost 40 years after its conception, FRAP is has become a mature technique that is of great value to pharmaceutical research. The technique has been employed to tailor the properties of drug delivery systems, to test how drugs can overcome delivery barriers inside the body, to improve several medical therapies, and even to serve as a diagnostic tool.

The success of FRAP has several explanations. First of all, the technique is conceptually simple and in recent years widely available to everyone with access to a standard CLSM. Secondly, it is one of the few tools that is able to perform diffusion measurements inside living tissue and even inside living cells. This is an invaluable asset to pharmaceutical research and more generally to the life sciences. And last but not least, FRAP is a versatile technique, not being limited to measuring diffusion coefficients, but also allowing investigation of binding kinetics, membrane fluidity, gap junctional intracellular communication, and permeability of vesicles.

Despite the success of FRAP, some critical remarks are in place. Most theoretical FRAP models make some stringent assumptions that are hard to meet in some situations. This might not be much of an issue in simple drug delivery systems like hydrogels, but problems can arise in more complicated biological systems. For instance, inside living cells, deviations in the fluorescence recovery caused by the cell boundaries cannot easily be corrected for. However, most other problems can be avoided by choosing an appropriate (but usually also more complicated) FRAP model. Apart from these theoretical issues, another important but underreported problem when performing FRAP in living systems is the amount of damage caused by photobleaching and the possible related increase in temperature (119). These effects should be minimized as much as possible since they can distort the measurements.

Besides FRAP, other fluorescence techniques exist that are capable of diffusion measurements. In particular, raster image correlation spectroscopy (RICS), fluorescence correlation spectroscopy (FCS) and single particle tracking (SPT) are interesting alternative techniques that do not suffer from some of the drawbacks listed above, simply because they do not rely on deliberate photobleaching (41, 120-122) . For some applications, FRAP might become replaced by FCS, RICS, or SPT, but as they have their own limitations, FRAP will continue to be of use to pharmaceutical research because of its obvious advantages.

References

1. D.Axelrod, D.E.Koppel, J.Schlessinger, E.Elson, and W.W.Webb. Mobility Measurement by Analysis of Fluorescence Photobleaching Recovery Kinetics. Biophysical Journal. 16:1055-1069 (1976).

2. J.Schlessinger, D.E.Koppel, D.Axelrod, K.Jacobson, W.W.Webb, and E.L.Elson. Lateral Transport on Cell-Membranes - Mobility of Concanavalin A Receptors on Myoblasts. Proceedings of the National Academy of Sciences of the United States of America. 73:2409-2413 (1976).

3. M.Edidin, Y.Zagyansky, and T.J.Lardner. Measurement of Membrane Protein Lateral Diffusion in Single Cells. Science. 191:466-468 (1976).

4. Y.Wang, F.Lanni, P.L.Mcneil, B.R.Ware, and D.L.Taylor. Mobility of Cytoplasmic and Membrane-Associated Actin in Living Cells. Proceedings of the National Academy of Sciences of the United States of America-Biological Sciences. 79:4660-4664 (1982).

5. J.W.Wojcieszyn, R.A.Schlegel, E.S.Wu, and K.A.Jacobson. Diffusion of Injected Macromolecules Within the Cytoplasm of Living Cells. Proceedings of the National Academy of Sciences of the United States of America-Biological Sciences. 78:4407-4410 (1981).

6. H.G.Kapitza, G.Mcgregor, and K.A.Jacobson. Direct Measurement of Lateral Transport in Membranes by Using Time-Resolved Spatial Photometry. Proceedings of the National Academy of Sciences of the United States of America. 82:4122-4126 (1985).

7. S.R.Chary and R.K.Jain. Direct Measurement of Interstitial Convection and Diffusion of Albumin in Normal and Neoplastic Tissues by Fluorescence Photobleaching. Proceedings of the National Academy of Sciences of the United States of America. 86:5385-5389 (1989).

8. D.A.Berk, F.Yuan, M.Leunig, and R.K.Jain. Fluorescence Photobleaching with Spatial Fourier-Analysis - Measurement of Diffusion in Light-Scattering Media. Biophysical Journal. 65:2428-2436 (1993).

9. W.M.Saltzman, M.L.Radomsky, K.J.Whaley, and R.A.Cone. Antibody Diffusion in Human Cervical-Mucus. Biophysical Journal. 66:508-515 (1994).

10. E.N.Kaufman and R.K.Jain. Quantification of Transport and Binding Parameters Using Fluorescence Recovery After Photobleaching - Potential for Invivo Applications. Biophysical Journal. 58:873-885 (1990).

11. K.Braeckmans, S.C.De Smedt, M.Leblans, R.Pauwels, and J.Demeester. Encoding microcarriers: Present and future technologies. Nature Reviews Drug Discovery. 1:447-456 (2002).

12. K.Braeckmans, S.C.De Smedt, C.Roelant, M.Leblans, R.Pauwels, and J.Demeester. Encoding microcarriers by spatial selective photobleaching. Nature Materials. 2:169-173 (2003).

13. E.B.Brown, E.S.Wu, W.Zipfel, and W.W.Webb. Measurement of molecular diffusion in solution by multiphoton fluorescence photobleaching recovery. Biophysical Journal. 77:2837-2849 (1999).

14. D.Mazza, K.Braeckmans, F.Cella, I.Testa, D.Vercauteren, J.Demeester, S.S.De Smedt, and A.Diaspro. A new FRAP/FRAPa method for three-dimensional diffusion measurements based on multiphoton excitation microscopy. Biophysical Journal. 95:3457-3469 (2008).

15. J.G.McNally, W.G.Muller, D.Walker, R.Wolford, and G.L.Hager. The glucocorticoid receptor: Rapid exchange with regulatory sites in living cells. Science. 287:1262-1265 (2000).

16. R.Swaminathan, C.P.Hoang, and A.S.Verkman. Photobleaching recovery and anisotropy decay of green fluorescent protein GFP-S65T in solution and cells: Cytoplasmic viscosity probed by green fluorescent protein translational and rotational diffusion. Biophysical Journal. 72:1900-1907 (1997).

17. J.White and E.Stelzer. Photobleaching GFP reveals protein dynamics inside live cells. Trends in Cell Biology. 9:61-65 (1999).

18. T.K.L.Meyvis, S.C.De Smedt, P.Van Oostveldt, and J.Demeester. Fluorescence recovery after photobleaching: A versatile tool for mobility and interaction measurements in pharmaceutical research. Pharmaceutical Research. 16:1153-1162 (1999).

19. A.S.Verkman. Solute and macromolecule diffusion in cellular aqueous compartments. Trends in Biochemical Sciences. 27:27-33 (2002).

20. U.Kubitscheck, P.Wedekind, and R.Peters. Three-dimensional diffusion measurements by scanning microphotolysis. Journal of Microscopy-Oxford. 192:126-138 (1998).

21. T.T.Tsay and K.A.Jacobson. Spatial Fourier-Analysis of Video Photobleaching Measurements - Principles and Optimization. Biophysical Journal. 60:360-368 (1991).

22. H.Deschout, J.Hagman, S.Fransson, J.Jonasson, M.Rudemo, N.Loren, and K.Braeckmans. Straightforward FRAP for quantitative diffusion measurements with a laser scanning microscope. Optics Express. 18:22886-22905 (2010).

23. J.K.Jonasson, J.Hagman, N.Loren, D.Bernin, M.Nyden, and M.Rudemo. Pixel-based analysis of FRAP data with a general initial bleaching profile. Journal of Microscopy. 239:142-153 (2010).

24. P.Jonsson, M.P.Jonsson, J.O.Tegenfeldt, and F.Hook. A Method Improving the Accuracy of Fluorescence Recovery after Photobleaching Analysis. Biophysical Journal. 95:5334-5348 (2008).

25. H.G.Kapitza, G.Mcgregor, and K.A.Jacobson. Direct Measurement of Lateral Transport in Membranes by Using Time-Resolved Spatial Photometry. Proceedings of the National Academy of Sciences of the United States of America. 82:4122-4126 (1985).

26. J.Crank. The Mathematics of Diffusion, Oxford University Press, Oxford, 1975.

27. D.M.Soumpasis. Theoretical-Analysis of Fluorescence Photobleaching Recovery Experiments. Biophysical Journal. 41:95-97 (1983).

28. J.K.Jonasson, N.Loren, P.Olofsson, M.Nyden, and M.Rudemo. A pixel-based likelihood framework for analysis of fluorescence recovery after photobleaching data. Journal of Microscopy. 232:260-269 (2008).

29. K.Braeckmans, L.Peeters, N.N.Sanders, S.C.De Smedt, and J.Demeester. Three-dimensional fluorescence recovery after photobleaching with the confocal scanning laser microscope. Biophysical Journal. 85:2240-2252 (2003).

30. U.Kubitscheck, P.Wedekind, and R.Peters. Lateral Diffusion Measurement at High-Spatial-Resolution by Scanning Microphotolysis in A Confocal Microscope. Biophysical Journal. 67:948-956 (1994).

31. S.Seiffert and W.Oppermann. Systematic evaluation of FRAP experiments performed in a confocal laser scanning microscope. Journal of Microscopy-Oxford. 220:20-30 (2005).

32. K.Braeckmans, B.G.Stubbe, K.Remaut, J.Demeester, and S.C.De Smedt. Anomalous photobleaching in fluorescence recovery after photobleaching measurements due to excitation saturation- a case study for fluorescein. Journal of Biomedical Optics. 11 (2006).

33. P.Wedekind, U.Kubitscheck, O.Heinrich, and R.Peters. Line-scanning microphotolysis for diffraction-limited measurements of lateral diffusion. Biophysical Journal. 71:1621-1632 (1996).

34. A.Tannert, S.Tannert, S.Burgold, and M.Schaefer. Convolution-based one and two component FRAP analysis: theory and application. European Biophysics Journal with Biophysics Letters. 38:649-661 (2009).

35. B.L.Sprague, R.L.Pego, D.A.Stavreva, and J.G.McNally. Analysis of binding reactions by fluorescence recovery after photobleaching. Biophysical Journal. 86:3473-3495 (2004).

36. F.Mueller, D.Mazza, T.J.Stasevich, and J.G.McNally. FRAP and kinetic modeling in the analysis of nuclear protein dynamics: what do we really know? Current Opinion in Cell Biology. 22:403-411 (2010).

37. J.Lippincott-Schwartz, N.tan-Bonnet, and G.H.Patterson. Photobleaching and photoactivation: following protein dynamics in living cells. Nature Cell Biology:S7-S14 (2003).

38. P.Van Oostveldt and S.Bauwens. Quantitative Fluorescence in Confocal Microscopy - the Effect of the Detection Pinhole Aperture on the Reabsorption and Inner Filter Phenomena. Journal of Microscopy-Oxford. 158:121-132 (1990).

39. F.Cella and A.Diaspro. Two-Photon Excitation Microscopy: A Superb Wizard for Fluorescence Imaging. In A.Diaspro (ed.), Nanoscopy and Multidimensional Optical Fluorescence Microscopy, Chapman & Hall, Boca Raton, 2010.

40. J.Braga, J.M.P.Desterro, and M.Carmo-Fonseca. Intracellular macromolecular mobility measured by fluorescence recovery after photobleaching with confocal laser scanning microscopes. Molecular Biology of the Cell. 15:4749-4760 (2004).

41. J.R.Thiagarajah, J.K.Kim, M.Magzoub, and A.S.Verkman. Slowed diffusion in tumors revealed by microfiberoptic epifluorescence photobleaching. Nat Methods. 3:275-280 (2006).

42. J.Wu, N.Shekhar, P.P.Lele, and T.P.Lele. FRAP Analysis: Accounting for Bleaching during Image Capture. Plos One. 7 (2012).

43. W.E.Hennink and C.F.van Nostrum. Novel crosslinking methods to design hydrogels. Advanced Drug Delivery Reviews. 54:13-36 (2002).

44. T.Vermonden, R.Censi, and W.E.Hennink. Hydrogels for Protein Delivery. Chemical Reviews. 112:2853-2888 (2012).

45. M.C.Branco, D.J.Pochan, N.J.Wagner, and J.P.Schneider. Macromolecular diffusion and release from self-assembled beta-hairpin peptide hydrogels. Biomaterials. 30:1339-1347 (2009).

46. S.R.Van Tomme, B.G.De Geest, K.Braeckmans, S.C.De Smedt, F.Siepmann, J.Siepmann, C.F.van Nostrum, and W.E.Hennink. Mobility of model proteins in hydrogels composed of oppositely charged dextran microspheres studied by protein release and fluorescence recovery after photobleaching. Journal of Controlled Release. 110:67-78 (2005).

47. F.Brandl, F.Kastner, R.M.Gschwind, T.Blunk, J.Tessmar, and A.Gopferich. Hydrogel-based drug delivery systems: Comparison of drug diffusivity and release kinetics. Journal of Controlled Release. 142:221-228 (2010).

48. M.Henke, F.Brandl, A.M.Goepferich, and J.K.Tessmar. Size-dependent release of fluorescent macromolecules and nanoparticles from radically cross-linked hydrogels. European Journal of Pharmaceutics and Biopharmaceutics. 74:184-192 (2010).

49. L.Payet, A.Ponton, L.Leger, H.Hervet, J.L.Grossiord, and F.Agnely. Self-Diffusion in Chitosan Networks: From a Gel-Gel Method to Fluorescence Recovery after Photobleaching by Fringe Pattern. Macromolecules. 41:9376-9381 (2008).

50. K.B.Kosto and W.M.Deen. Diffusivities of macromolecules in composite hydrogels. Aiche Journal. 50:2648-2658 (2004).

51. A.J.Kuijpers, G.H.M.Engbers, T.K.L.Meyvis, S.S.C.de Smedt, J.Demeester, J.Krijgsveld, S.A.J.Zaat, J.Dankert, and J.Feijen. Combined gelatin-chondroitin sulfate hydrogels for controlled release of cationic antibacterial proteins. Macromolecules. 33:3705-3713 (2000).

52. R.Censi, T.Vermonden, M.J.van Steenbergen, H.Deschout, K.Braeckmans, S.C.De Smedt, C.F.van Nostrum, P.di Martino, and W.E.Hennink. Photopolymerized thermosensitive hydrogels for tailorable diffusion-controlled protein delivery. Journal of Controlled Release. 140:230-236 (2009).

53. T.Vermonden, S.S.Jena, D.Barriet, R.Censi, J.van der Gucht, W.E.Hennink, and R.A.Siegel. Macromolecular Diffusion in Self-Assembling Biodegradable Thermosensitive Hydrogels. Macromolecules. 43:782-789 (2010).

54. J.Kang and K.J.Beers. Macromolecular transport through nanostructured and porous hydrogels synthesized using the amphiphilic copolymer, PCL-b-PEO-b-PCL. European Polymer Journal. 45:3004-3009 (2009).

55. M.D.Burke, J.O.Park, M.Srinivasarao, and S.A.Khan. A novel enzymatic technique for limiting drug mobility in a hydrogel matrix. Journal of Controlled Release. 104:141-153 (2005).

56. F.Alvarez-Mancenido, K.Braeckmans, S.C.De Smedt, J.Demeester, M.Landin, and R.Martinez-Pacheco. Characterization of diffusion of macromolecules in konjac glucomannan solutions and gels by fluorescence recovery after photobleaching technique. International Journal of Pharmaceutics. 316:37-46 (2006).

57. R.Xiong, S.Soenen, K.Braeckmans, and A.G.Skirtach. Towards Theranostic Multicompartment Microcapsules: in-situ Diagnostics and Laser-induced Treatment. Theranostics. 3:141-151 (2013).

58. K.Kohler and G.B.Sukhorukov. Heat treatment of polyelectrolyte multilayer capsules: A versatile method for encapsulation. Advanced Functional Materials. 17:2053-2061 (2007).

59. M.S.Toprak, B.J.McKenna, J.H.Waite, and G.D.Stucky. Control of size and permeability of nanocomposite microspheres. Chemistry of Materials. 19:4263-4269 (2007).

60. X.Tao, X.J.Sun, J.M.Su, J.F.Chen, and W.Roa. Natural microshells of alginate-chitosan: Unexpected stability and permeability. Polymer. 47:6167-6171 (2006).

61. Y.Cheng, R.K.Prud'homme, and J.L.Thomas. Diffusion of mesoscopic probes in aqueous polymer solutions measured by fluorescence recovery after photobleaching. Macromolecules. 35:8111-8121 (2002).

62. S.Basu and P.J.Campagnola. Properties of crosslinked protein matrices for tissue engineering applications synthesized by multiphoton excitation. Journal of Biomedical Materials Research Part A. 71A:359-368 (2004).

63. K.Remaut, N.N.Sanders, B.G.De Geest, K.Braeckmans, J.Demeester, and S.C.De Smedt. Nucleic acid delivery: Where material sciences and bio-sciences meet. Materials Science & Engineering R-Reports. 58:117-161 (2007).

64. A.Pluen, Y.Boucher, S.Ramanujan, T.D.Mckee, T.Gohongi, E.di Tomaso, E.B.Brown, Y.Izumi, R.B.Campbell, D.A.Berk, and R.K.Jain. Role of tumor-host interactions in interstitial diffusion of macromolecules: Cranial vs. subcutaneous tumors. Proceedings of the National Academy of Sciences of the United States of America. 98:4628-4633 (2001).

65. P.A.Netti, D.A.Berk, M.A.Swartz, A.J.Grodzinsky, and R.K.Jain. Role of extracellular matrix assembly in interstitial transport in solid tumors. Cancer Research. 60:2497-2503 (2000).

66. S.Ramanujan, A.Pluen, T.D.Mckee, E.B.Brown, Y.Boucher, and R.K.Jain. Diffusion and convection in collagen gels: Implications for transport in the tumor interstitium. Biophysical Journal. 83:1650-1660 (2002).

67. T.Stylianopoulos, B.op-Frimpong, L.L.Munn, and R.K.Jain. Diffusion Anisotropy in Collagen Gels and Tumors: The Effect of Fiber Network Orientation. Biophysical Journal. 99:3119-3128 (2010).

68. A.Erikson, H.N.Andersen, S.N.Naess, P.Sikorski, and C.D.Davies. Physical and chemical modifications of collagen gels: Impact on diffusion. Biopolymers. 89:135-143 (2008).

69. L.Eikenes, I.Tufto, E.A.Schnell, A.Bjorkoy, and C.D.Davies. Effect of Collagenase and Hyaluronidase on Free and Anomalous Diffusion in Multicellular Spheroids and Xenografts. Anticancer Research. 30:359-368 (2010).

70. V.P.Chauhan, R.M.Lanning, B.op-Frimpong, W.Mok, E.B.Brown, T.P.Padera, Y.Boucher, and R.K.Jain. Multiscale Measurements Distinguish Cellular and Interstitial Hindrances to Diffusion In Vivo. Biophysical Journal. 97:330-336 (2009).

71. M.Magzoub, S.Jin, and A.S.Verkman. Enhanced macromolecule diffusion deep in tumors after enzymatic digestion of extracellular matrix collagen and its associated proteoglycan decorin. Faseb Journal. 22:276-284 (2008).

72. K.D.Sullivan, W.H.Sipprell, E.B.Brown, and E.B.Brown. Improved Model of Fluorescence Recovery Expands the Application of Multiphoton Fluorescence Recovery after Photobleaching in Vivo. Biophysical Journal. 96:5082-5094 (2009).

73. D.K.Binder, M.C.Papadopoulos, P.M.Haggie, and A.S.Verkman. In vivo measurement of brain extracellular space diffusion by cortical surface photobleaching. Journal of Neuroscience. 24:8049-8056 (2004).

74. E.Sykova and C.Nicholson. Diffusion in brain extracellular space. Physiological Reviews. 88:1277-1340 (2008).

75. M.C.Papadopoulos, D.K.Binder, and A.S.Verkman. Enhanced macromolecular diffusion in brain extracellular space in mouse models of vasogenic edema measured by cortical surface photobleaching. Faseb Journal. 18:425-+ (2004).

76. M.C.Papadopoulos, J.K.Kim, and A.S.Verkman. Extracellular space diffusion in central nervous system: Anisotropic diffusion measured by elliptical surface photobleaching. Biophysical Journal. 89:3660-3668 (2005).

77. Z.Zador, M.Magzoub, S.Jin, G.T.Manley, M.C.Papadopoulos, and A.S.Verkman. Microfiberoptic fluorescence photobleaching reveals size-dependent macromolecule diffusion in extracellular space deep in brain. Faseb Journal. 22:870-879 (2008).

78. N.N.Sanders, S.C.De Smedt, and J.Demeester. The physical properties of biogels and their permeability for macromolecular drugs and colloidal drug carriers. Journal of Pharmaceutical Sciences. 89:835-849 (2000).

79. P.Occhipinti and P.C.Griffiths. Quantifying diffusion in mucosal systems by pulsed-gradient spin-echo NMR. Advanced Drug Delivery Reviews. 60:1570-1582 (2008).

80. S.S.Olmsted, J.L.Padgett, A.I.Yudin, K.J.Whaley, T.R.Moench, and R.A.Cone. Diffusion of macromolecules and virus-like particles in human cervical mucus. Biophysical Journal. 81:1930-1937 (2001).

81. H.Shen, Y.Y.Hu, and W.M.Saltzman. DNA diffusion in mucus: Effect of size, topology of DNAs, and transfection reagents. Biophysical Journal. 91:639-644 (2006).

82. E.H.Burger and J.Klein-Nulend. Mechanotransduction in bone - role of the lacuno-canalicular network. Faseb Journal. 13:S101-S112 (1999).

83. X.Z.Zhou, J.E.Novotny, and L.Y.Wang. Modeling Fluorescence Recovery After Photobleaching in Loaded Bone: Potential Applications in Measuring Fluid and Solute Transport in the Osteocytic Lacunar-Canalicular System. Annals of Biomedical Engineering. 36:1961-1977 (2008).

84. C.Price, X.Z.Zhou, W.Li, and L.Y.Wang. Real-Time Measurement of Solute Transport Within the Lacunar-Canalicular System of Mechanically Loaded Bone: Direct Evidence for Load-Induced Fluid Flow. Journal of Bone and Mineral Research. 26:277-285 (2011).

85. L.Peeters, N.N.Sanders, K.Braeckmans, K.Boussery, J.V.de Voorde, S.C.De Smedt, and J.Demeester. Vitreous: A barrier to nonviral ocular gene therapy. Investigative Ophthalmology & Visual Science. 46:3553-3561 (2005).

86. M.E.Johnson, D.A.Berk, D.Blankschtein, D.E.Golan, R.K.Jain, and R.S.Langer. Lateral diffusion of small compounds in human stratum corneum and model lipid bilayer systems. Biophysical Journal. 71:2656-2668 (1996).

87. O.Seksek, J.Biwersi, and A.S.Verkman. Translational diffusion of macromolecule-sized solutes in cytoplasm and nucleus. Journal of Cell Biology. 138:131-142 (1997).

88. M.ArrioDupont, S.Cribier, G.Foucault, P.F.Devaux, and A.d'Albis. Diffusion of fluorescently labeled macromolecules in cultured muscle cells. Biophysical Journal. 70:2327-2332 (1996).

89. M.ArrioDupont, G.Foucault, M.Vacher, P.F.Devaux, and S.Cribier. Translational diffusion of globular proteins in the cytoplasm of cultured muscle cells. Biophysical Journal. 78:901-907 (2000).

90. E.Moeendarbary, L.Valon, M.Fritzsche, A.R.Harris, D.A.Moulding, A.J.Thrasher, E.Stride, L.Mahadevan, and G.T.Charras. The cytoplasm of living cells behaves as a poroelastic material. Nature Materials. 12:253-261 (2013).

91. G.L.Lukacs, P.Haggie, O.Seksek, D.Lechardeur, N.Freedman, and A.S.Verkman. Size-dependent DNA mobility in cytoplasm and nucleus. Journal of Biological Chemistry. 275:1625-1629 (2000).

92. J.C.Politz, E.S.Browne, D.E.Wolf, and T.Pederson. Intranuclear diffusion and hybridization state of oligonucleotides measured by fluorescence correlation spectroscopy in living cells. Proceedings of the National Academy of Sciences of the United States of America. 95:6043-6048 (1998).

93. A.T.Jones and E.J.Sayers. Cell entry of cell penetrating peptides: tales of tails wagging dogs. Journal of Controlled Release. 161:582-591 (2012).

94. F.Cardarelli, M.Serresi, R.Bizzarri, M.Giacca, and F.Beltram. In vivo study of HIV-1 Tat arginine-rich motif unveils its transport properties. Molecular Therapy. 15:1313-1322 (2007).

95. M.J.Roberti, T.M.Jovin, and E.Jares-Erijman. Confocal Fluorescence Anisotropy and FRAP Imaging of alpha-Synuclein Amyloid Aggregates in Living Cells. Plos One. 6 (2011).

96. N.J.Edwin, R.P.Hammer, R.L.McCarley, and P.S.Russo. Reversibility of beta-Amyloid Self-Assembly: Effects of pH and Added Salts Assessed by Fluorescence Photobleaching Recovery. Biomacromolecules. 11:341-347 (2010).

97. I.Sponne, A.Fifre, A.Drouet, C.Klein, V.Koziel, M.Pingon-Raymond, J.L.Olivier, J.Chambaz, and T.Pillot. Apoptotic neuronal cell death induced by the non-fibrillar amyloid-beta peptide proceeds through an early reactive oxygen species-dependent cytoskeleton perturbation. Journal of Biological Chemistry. 278:3437-3445 (2003).

98. K.Guan, S.Wagner, B.Unsold, L.S.Maier, D.Kaiser, B.Hemmerlein, K.Nayernia, W.Engel, and G.Hasenfuss. Generation of functional cardiomyocytes from adult mouse spermatogonial stem cells. Circulation Research. 100:1615-1625 (2007).

99. B.J.Muller-Borer, W.E.Cascio, P.A.W.Anderson, J.N.Snowwaert, J.R.Frye, N.Desai, G.L.Esch, J.A.Brackham, C.R.Bagnell, W.B.Coleman, J.W.Grisham, and N.N.Malouf. Adult-derived liver

stem cells acquire a cardiomyocyte structural and functional phenotype ex vivo. American Journal of Pathology. 165:135-145 (2004).

100. M.G.Todorova, B.Soria, and I.Quesada. Gap junctional intercellular communication is required to maintain embryonic stem cells in a non-differentiated and proliferative state. Journal of Cellular Physiology. 214:354-362 (2008).

101. Y.Y.Lu, T.S.Chen, X.P.Wang, and L.Li. Single-cell analysis of dihydroartemisinin-induced apoptosis through reactive oxygen species-mediated caspase-8 activation and mitochondrial pathway in ASTC-a-1 cells using fluorescence imaging techniques. Journal of Biomedical Optics. 15 (2010).

102. X.H.Long, M.Y.Fan, R.M.Bigsby, and K.P.Nephew. Apigenin inhibits antiestrogen-resistant breast cancer cell growth through estrogen receptor-alpha-dependent and estrogen receptor-alpha-independent mechanisms. Molecular Cancer Therapeutics. 7:2096-2108 (2008).

103. M.S.Phadke, N.F.Krynetskaia, A.K.Mishra, and E.Krynetskiy. Glyceraldehyde 3-Phosphate Dehydrogenase Depletion Induces Cell Cycle Arrest and Resistance to Antimetabolites in Human Carcinoma Cell Lines. Journal of Pharmacology and Experimental Therapeutics. 331:77-86 (2009).

104. L.Sancey, E.Garanger, S.Foillard, G.Schoehn, A.Hurbin, C.biges-Rizo, D.Boturyn, C.Souchier, A.Grichine, P.Dumy, and J.L.Coll. Clustering and Internalization of Integrin alpha(v)beta(3) With a Tetrameric RGD-synthetic Peptide. Molecular Therapy. 17:837-843 (2009).

105. D.A.Berk, F.Yuan, M.Leunig, and R.K.Jain. Direct in vivo measurement of targeted binding in a human tumor xenograft. Proceedings of the National Academy of Sciences of the United States of America. 94:1785-1790 (1997).

106. E.N.Kaufman and R.K.Jain. Effect of Bivalent Interaction Upon Apparent Antibody-Affinity - Experimental Confirmation of Theory Using Fluorescence Photobleaching and Implications for Antibody-Binding Assays. Cancer Research. 52:4157-4167 (1992).

107. T.Ogawa, T.Hayashi, M.Tokunou, K.Nakachi, J.E.Trosko, C.C.Chang, and N.Yorioka. Suberoylanilide hydroxamic acid enhances gap junctional intercellular communication via acetylation of histone containing Connexin 43 gene locus. Cancer Research. 65:9771-9778 (2005).

108. H.Sauer, V.Putz, K.Fischer, J.Hescheler, and M.Wartenberg. Increased doxorubicin uptake and toxicity in multicellular tumour spheroids treated with DC electrical fields. British Journal of Cancer. 80:1204-1213 (1999).

109. M.J.C.Machado and C.A.Mitchell. Temporal changes in microvessel leakiness during wound healing discriminated by in vivo fluorescence recovery after photobleaching. Journal of Physiology-London. 589:4681-4696 (2011).

110. T.Da and A.S.Verkman. Aquaporin-4 gene disruption in mice protects against impaired retinal function and cell death after ischemia. Investigative Ophthalmology & Visual Science. 45:4477-4483 (2004).

111. J.A.van Aalst, W.Burmeister, P.L.Fox, and L.M.Graham. alpha-Tocopherol preserves endothelial cell migration in the presence of cell-oxidized low-density lipoprotein by inhibiting changes in cell membrane fluidity. Journal of Vascular Surgery. 39:229-237 (2004).

112. G.Jones, F.Hunter, H.A.Hancock, A.Kapoor, M.J.Stone, B.J.Wood, J.W.Xie, M.R.Dreher, and V.Frenkel. In Vitro Investigations Into Enhancement of tPA Bioavailability in Whole Blood Clots Using Pulsed-High Intensity Focused Ultrasound Exposures. Ieee Transactions on Biomedical Engineering. 57:33-36 (2010).

113. D.Salinas, P.M.Haggie, J.R.Thiagarajah, Y.L.Song, K.Rosbe, W.E.Finkbeiner, D.W.Nielson, and A.S.Verkman. Submucosal gland dysfunction as a primary defect in cystic fibrosis. Faseb Journal. 18:431-+ (2004).

114. C.M.Finnegan, S.S.Rawat, E.H.Cho, D.L.Guiffre, S.Lockett, A.H.Merrill, and R.Blumenthal. Sphingomyelinase restricts the lateral diffusion of CD4 and inhibits human immunodeficiency virus fusion. Journal of Virology. 81:5294-5304 (2007).

115. R.Lin, R.Murtazina, B.Y.Cha, M.Chakraborty, R.Sarker, T.E.Chen, Z.H.Lin, B.M.Hogema, H.R.de Jonge, U.Seidler, J.R.Turner, X.H.Li, O.Kovbasnjuk, and M.Donowitz. D-Glucose Acts via Sodium/Glucose Cotransporter 1 to Increase NHE3 in Mouse Jejunal Brush Border by a Na plus/H plus Exchange Regulatory Factor 2-Dependent Process. Gastroenterology. 140:560-571 (2011).

116. R.Saxena and A.Chattopadhyay. Membrane organization and dynamics of the serotonin(1A) receptor in live cells. Journal of Neurochemistry. 116:726-733 (2011).

117. E.Meimaridou, S.B.Gooljar, N.Ramnarace, L.Anthonypillai, A.J.L.Clark, and J.P.Chapple. The Cytosolic Chaperone Hsc70 Promotes Traffic to the Cell Surface of Intracellular Retained Melanocortin-4 Receptor Mutants. Molecular Endocrinology. 25:1650-1660 (2011).

118. A.Gefen, L.H.Cornelissen, D.Gawlitta, D.L.Bader, and C.W.J.Oomens. The free diffusion of macromolecules in tissue-engineered skeletal muscle subjected to large compression strains. Journal of Biomechanics. 41:845-853 (2008).

119. J.W.Dobrucki, D.Feret, and A.Noatynska. Scattering of exciting light by live cells in fluorescence Confocal imaging: Phototoxic effects and relevance for FRAP studies. Biophysical Journal. 93:1778-1786 (2007).

120. C.M.Brown, R.B.Dalal, B.Hebert, M.A.Digman, A.R.Horwitz, and E.Gratton. Raster image correlation spectroscopy (RICS) for measuring fast protein dynamics and concentrations with a commercial laser scanning confocal microscope. J Microsc. 229:78-91 (2008).

121. S.T.Hess, S.H.Huang, A.A.Heikal, and W.W.Webb. Biological and chemical applications of fluorescence correlation spectroscopy: A review. Biochemistry. 41:697-705 (2002).

122. M.J.Saxton and K.Jacobson. Single-particle tracking: Applications to membrane dynamics. Annual Review of Biophysics and Biomolecular Structure. 26:373-399 (1997).